



Design of acoustic coating for underwater stealth in low-frequency ranges

Mostafa Ranjbar¹ · Muhammed Umar Bayer²

Received: 23 October 2023 / Accepted: 15 January 2024 / Published online: 20 February 2024
© The Author(s) 2024

Abstract

In this study, it is aimed to protect underwater vehicles against active sonar systems by anechoic coating. A matrix material with close acoustic impedance to water, resistivity to hydrostatic pressure, suitability for the marine environment, and high material loss factor is selected. At low frequencies, the inclusions in different shapes and sizes are added to the matrix material. Since solid inclusions will increase the coating mass considerably, air cavities are preferred as inclusions. More attention is paid to low-frequency absorption, especially below 1 kHz, because of advancing sonar technology. The acoustic performance of the designed models is compared in three frequency ranges: low (below 3 kHz), middle (3–6 kHz), and high (6–10 kHz). The designed models are constructed by considering hydrostatic pressure; hence, volume of air cavities is tried to decrease, while absorption performance is aimed to increase. Therefore, a conical cavity which commonly used in the literature is optimized by changing its dimensions and location. Also, novel approaches, gong shape cavity, and sandglass cavities are introduced. The results show that, not only cavity shape, but also its location and dimensions are highly influential on absorption performance. High-volume cavities increase the absorption performance at the low-frequency range, but they are not effective at high frequencies. The gong shape and sandglass air cavities show broadband absorption; also, gong shape cavity volume is less than literature models. Thus, its usability increases at deep waters. The results of this study provide novel underwater acoustic coating models for various applications.

Keywords Underwater · Acoustic · Coating · Stealth · Low frequency

1 Introduction

Metamaterials are novel artificial structures which show extraordinary features. The research about metamaterials began in optics and electrodynamics fields in the 1990s. The publications in the 2000s [1, 2] could be considered as first studies in the acoustic field. Acoustic metamaterials (AM) have been widely studying for a long time, and application areas are expanding. Acoustic absorption materials were

improved to reduce mechanical sounds, especially arising from aircrafts and cars up to the twentieth century. On the other hand, acoustic science finds novel application areas such as underwater, structural acoustics, automotive, and aviation [3–7]. The first anechoic structures could be considered as German submarines rubber coatings during World War II [8].

Designing novel acoustic absorption structures accelerates with the technological advance in the field of sonar technology. Nowadays, acoustic absorption materials have been researched widely in many contents [9, 10]. In particular, studies in acoustic metamaterials are focused on underwater applications; most of them aim to obtain high acoustic absorption in wide-frequency range. However, high absorption is shown only near zone of locally resonant frequencies in a narrowband. This problem could be solved by using layered structure. Each layer has a unique resonant frequency. Hence, the complete material has different several resonant frequencies. By this way, acoustic absorption performance

Technical Editor: Samikkannu Raja.

✉ Mostafa Ranjbar
mostafa.ranjbar@cranfield.ac.uk
Muhammed Umar Bayer
mbayer@bandirma.edu.tr

¹ Centre for Energy Engineering, School of Water Energy and Environment, Cranfield University, Cranfield, UK

² Naval Architecture and Marine Engineering, Bandırma Onyedi University, Bandırma, Turkey

could be enhanced. Also, by adding air cavities and metal powders, acoustic performance could be improved.

On the other hand, the probability of a fiber-reinforced structure being visible to the sonar is very low. Therefore, engineers who want to turn gigantic submarines into ghosts prefer plastic materials, rubber-like materials, or other special surface coatings. Thus, they prevent the reflection of acoustic signals and ensure that they are dispersed in all directions. For underwater acoustic absorption, polymers have been a traditional material. Except its high damping properties and close acoustic impedance to water, they have high resistance to water, corrosion, and abrasion, also, high thermal and electrical insulation [11]. Polymers are effective absorption materials with a certain frequency level. Moreover, broadband acoustic absorption could not be achieved yet by these novel materials especially below 100 Hz [12]. To obtain high acoustic absorption at low frequencies, mostly used approaches contain air cavities [13], metal filler [14], and polymers [15].

Gao et al. [14] designed a metamaterial which consists of conical air cavity, metal filler, and backing steel. They aimed to obtain high acoustic absorption at low frequencies. They selected the matrix material as viscoelastic rubber because of its high damping properties. Moreover, metal filler enhances the longitudinal to shear wave transformations. The conical air cavity increases the acoustic absorption performance of metamaterial, especially, at low frequencies. They performed the analysis as 2D and 3D. Also, to verify the FEA model, the transfer matrix method is applied to the metamaterial. Wang et al. [16] proposed an underwater metamaterial layer which consists of several steel scatters and rubber as soft matrix material. The dimensions of scatters are set as parameters, and several parametric studies are done to reach high acoustic absorption performance. Also, effect of adding a metal backing to the metamaterial is investigated. Their results show that increasing number of scatters enhances the sound absorption in several frequency ranges. Yang et al. [17] proposed a novel hybrid metastructure design for underwater acoustic absorption which consists of air cavities and locally resonant metastructure. They proposed that the absorption performance of air embedded rubber with steel backing could be improved by the locally resonant metastructure. Their results show that locally resonant scatterers cause wave attenuation, inertial loss, and impedance matching with water. The combination of air cavities which are efficient at high frequencies, and locally resonant scatters which are efficient at low frequencies, provide broadband absorption performance. Jin et al. [18] proposed a novel underwater acoustic metamaterial which consists of air cavities and periodic multi-resonator which embedded in sound insulation and absorption layer, respectively. To optimize acoustic performance of slab, interior geometries of layers are arranged; finite element

method is utilized to obtain the absorption performance of slab. Firstly, they introduced two different combinations. The difference between these is location of flat steel plate; both models consist of epoxy, steel, and soft rubber. The cylindrical form steel plates which surrounded by soft rubber behave as different resonators. Therefore, it is expected to behave like a multi-resonator. Meng et al. [19] designed an anechoic slab based upon layers of locally resonant acoustic metamaterial (LRAM). They applied genetic algorithm to optimize underwater acoustic absorption of LRAM. They determined that layers of slab oscillate independently depending own resonant frequency. They determined that each layer of anechoic slab oscillate depending on resonant frequency, hence, proposed that independent oscillate modes occur. Their experimental and theoretical results indicate that various types of scatterers with different resonances enhance acoustic absorption characteristics in wide-frequency range. They determined that some parameters such as thickness of layers, lattice constants, and shape of scatterers are vital to optimization process of underwater anechoic layers. Wang et al. [20] designed a metastructure which consist of one and double microperforated panels with backing cavities (MPPB). They suggest that it provides high underwater acoustic absorption in wide-frequency range, especially, at low frequencies. Adding one more MPPB to the structure increases the number of absorption peaks at higher frequencies. However, at low frequencies, while the number of MPPB is increasing, absorption performance of the structure is nearly unchanged.

In this study, to pretend underwater vehicles against active sonar systems, an anechoic coating metamaterial is designed. Firstly, a matrix material is chosen that hosts the internal geometry. After, several air cavities with different shape, size, and location are added the matrix material. The significant factors are determined to be done parametric studies and optimization process. The finite element analyses are done as 3D via COMSOL Multiphysics 6.1 acoustic module.

2 Materials and method

Acoustic coatings could be fitted different parts of submarine hull such as bridge fin, pressure hull, and bridge casing according to needs. Also, there are several non-acoustic needs in naval architecture while fitting acoustic coating. They could be listed as, limited coating thickness (generally a few centimeters), density, and static compressibility, convenient thermal conductivity, resistance to environmental conditions, availability for gluing process, and fire resistance. Designed structure must be respond these requirements.

Table 1 Some materials with characteristic specific acoustic impedances [21]

Materials	Speed of sound (m/s)	Density (kg/m ³)	Impedance (Rayl)
Air	340	1.23	418
Water	1490	1053	1.56×10^6
Aluminum	6420	2690	1.73×10^7
PDMS	1119	969	1.08×10^6
Steel	5950	7860	4.64×10^7
Epoxy	2490	1180	2.95×10^6
PU	1040	1528	1.59×10^6
Ecoflex	989	1070	1.06×10^6

Table 2 Loss factors of some materials [23–25]

Materials	Loss factor
PDMS	≈ 0.15
Epoxy	≈ 0.039
Steel	$0.2 \sim 3 \times 10^{-4}$
Aluminum	$0.3 \sim 10 \times 10^{-5}$
PU	$\approx 0.05\text{--}0.15$

2.1 Underwater acoustic absorption mechanism

Polymers show high acoustic absorption performance due to their damping properties and close acoustic impedance to water. Characteristic specific impedances of some materials are shown in Table 1. Moreover, to enhance the acoustic performance of polymers, matrix materials, air cavities are quite helpful, especially at low frequencies. In polymers, incident wave acoustic energy is converted to heat and vibration; hence, the energy is dissipated.

The loss factor is defined as the ratio of imaginary part of phase angle to real part of phase angle [22] and increases loss factor result of high acoustic sound absorption in water domain. Table 2 shows the loss factors comparison with some materials using underwater acoustic applications and other materials. Adding inclusions to underwater metamaterial introduces additional mechanisms for underwater acoustic absorption such as friction, resonance, and wave mode conversion. Inclusions which embedded to matrix material have own natural frequencies; hence, as incident waves get closer to their natural frequency, metamaterial tends to resonance. Therefore, absorption peaks are shown with resonances.

The sound absorption coefficient of the anechoic coatings is calculated using the COMSOL Multiphysics TM 6.0, which is used to construct the numerical model. The matrix material and steel backing are represented as solid mechanics domains, whereas the water domain and cavities are represented as pressure acoustics domains. The cavities

are filled with air. The acoustic-solid coupling employs continuity boundary conditions at the interface between pressure acoustics and solid mechanics. Also, bottom side of the steel backing is set as low reflection boundary. Initial sound waves which generated with port section are plane waves. The material of backing steel properties is: Young's modulus $E = 3.6 \times 10^5$ (MPa), Poisson's ratio $\zeta = 0.28$. Polyurethane's Young's modulus and Poisson's ratio are 3.59 (MPa) and 0.49, respectively. Acoustic velocity, dynamic viscosity, and density of water are 1448 m/s, and 1.3 mPa.s, and 1000 kg/m³, respectively.

The acoustic pressure is determined by solving the Helmholtz equation given below:

$$\nabla^2 \left(\frac{p}{p_0} \right) + k^2 \frac{p}{p_0} = 0 \quad (1)$$

where p_0 is the density of water, p is sound pressure, $k = 2\pi f/c_0$ is wave number in a fluid medium, where c_0 and f represent sound velocity of water and frequency, and ∇ is the Laplacian operator.

The magnitude of the incident sound pressure is set to 1 Pa. The outer side of the steel backing and matrix material is chosen as the fixed constraint. Numerical simulation is used to compute the reflected sound pressure. The reflection coefficient R is determined by the following calculation,

$$R = \frac{p_r}{p_i} \quad (2)$$

where p_r , and p_i represent reflected and incident wave pressures, respectively.

Consequently, the absorption coefficient could be calculated as

$$\alpha = 1 - |R|^2 \quad (3)$$

2.2 Design and optimization

While designing the anechoic coating, studies in literature are based on [14, 26] and marine requests are considered such as density and water resistivity. Also, several dimensional concerns are examined in terms of submarine sailing. After that, the matrix material which hosts the internal air cavity is chosen as polyurethane, a kind of polymer due to its high damping features [27]. Frequently used coating materials are shown in Table 3.

The coating consists of unit cells. The external shape of the acoustic coating unit cell is designed as hexagon, and it shown in Fig. 1a. The hexagonal unit cells could be united without interior gaps. The bottom hexagon and the top hexagons represent the backing steel and water domain, respectively. The mid-hexagon is the matrix material PU. The backing steel and water domain thickness are set as 10 mm. The air cavities are placed in the PU (mid-hexagon). The

Table 3 Materials classes of country-based submarines [28, 29]

Country	Acoustic Coating Substrates
Germany	Composite rubber
USA	Polyurethane, glass fiber, butyl rubber
Russia	Styrene-butadiene rubber, polybutadiene rubber
France	Polyurethane, polysulfide rubber
UK	Polyurethane
Japan	Neoprene
China	Styrene-butadiene rubber, polyurethane

width of the one side of hexagon is set as 20 mm. Therefore, width of one-unit cell is 40 mm. Technical drawing of one of the designed models is shown in Fig. 1b. The dimensions are used as same representation in other models. The analyses are done by using the Bloch period boundary to three symmetric boundaries of hexagonal unit cell [14]. By this way, the computational time is reduced.

The distance between upper surface of first cavity and lower surface of water domain is represented as h_2 , and the distance from upper surface of second cavity and lower surface of water domain is represented as h_3 . The top and bottom radius of conical cavity are represented as r_1 and r_2 , respectively, and h_1 represents the length of conical cavity. The thickness of water domain and backing steel are represented as h_{water} and h_{steel} , respectively. Both are set as 10 mm in all models. The width of one-unit cell is 40 mm; a represents the half of the width of 20 mm. The thickness of matrix material is represented as h_{matrix} , and it is set as

30 mm in all models. The gong shape air cavity is obtained from the literature [30], and all dimensions are shown in Table 4.

2.3 Mesh sensitivity study

To obtain the ideal mesh quality, a mesh sensitivity study is conducted. Three types of mesh quality, namely Mesh-A (coarse), Mesh-B (medium), and Mesh-C (fine), are compared via gong shape cavity model ($h_3 = 22$ mm). For each three types of mesh, unstructured mesh type is utilized. It was observed that between A and B type mesh quality, approximately relative error (%) is between 0,11,054 and 0,360,586, and between B and C type is between 0,041272 and 0,101,758 for 1–10-kHz interval. Therefore, after C type mesh, there was no need to increase the mesh quality. Figure 2 shows the meshed bodies, and Table 5 shows the mesh quality-dependent absorption performance and approximately relative errors between different types of meshes. The detailed information about utilized mesh type, Mesh-C is given in Table 6.

3 Results and discussion

There are several parameters which affect the absorption performance of coating such as thickness of matrix material, form, dimensions, and location of air cavity. Firstly, in optimization section each parameter is examined separately. After determined the optimum value of each parameter, all

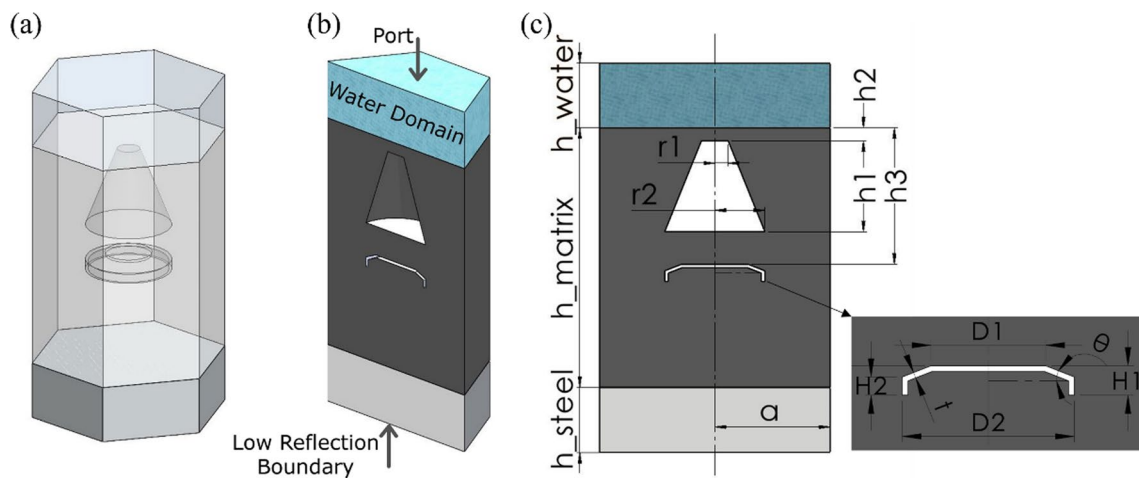


Fig. 1 a Hexagonal unit cell, b FEM model, and c technical drawing of basic unit cell

Table 4 Dimensions of the gong

Variable	H_1 (m)	H_2 (m)	D_1 (m)	D_2 (m)	t (m)	θ
Value	0.03	0.0145	0.0615	0.1125	0.002	15.87°

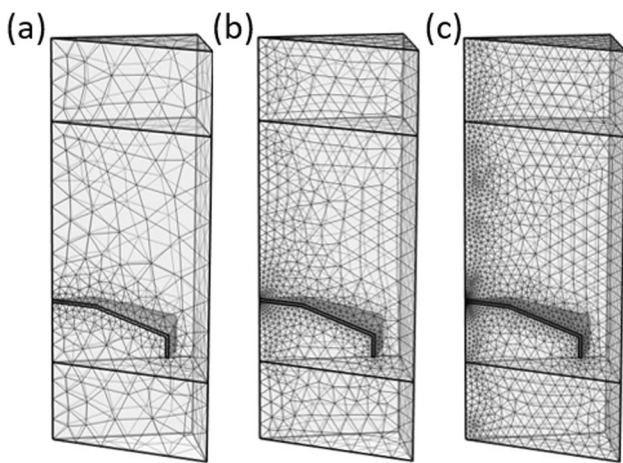


Fig. 2 a Mesh-A (coarse), b Mesh-B (medium), and c Mesh-C (fine) meshed bodies for gong shape cavity ($h_3 = 22$ mm)

parameters are examined together. So, the effect of each parameter on each other could be seen. Recently, absorber structure design met two concepts: soft coating and gradient medium [4]. The reflection coefficient of absorber tends to decrease with these two conditions. Soft coating is fulfilled by using PU and gradient mediums are used in the matrix material. After the material selection of matrix material is done, geometric conditions of cavity are examined. Air cavity could be in the cylindrical form; thus, absorption performance of pure PU could be enhanced. However, gradient condition is not satisfied with this form, and the absorption performance is limited. To obtain high absorption, cylindrical form is transformed into conical cavity form. The effect of the dimensions of conical cavity (top and bottom radius and thickness) and location of it, are analyzed. Firstly, the model which consists of pure PU with 30 mm thickness as matrix

material and backing steel is analyzed. Figure 3a shows the model and acoustic performance of this model.

Moreover, a conical cavity with 14 mm long with 1- and 15-mm top and bottom radius, respectively, is added to matrix material. The length and bottom radius of the cone kept constant, and the top radius of cone is set as 1, 4, 7, and 10 mm. The location of the top of cone is below 1 mm the water domain. The air domains are shown as blue. The acoustic performance of these parameters is shown in Fig. 3b. Also, the bottom radius of conical air cavity is considered as a significant parameter in terms of acoustic performance. Therefore, a parametric study is done which based on the bottom radius. The length, location, and top radius of the cone are kept constant, and bottom radius is set as 5, 10, 15, and 18 mm. The results of parametric study are shown in Fig. 3c. After, the top and bottom radius of conical air cavity kept constant, and length of cavity is set as 6, 10, 14, and 18 mm. The results of parametric study are shown in Fig. 3d.

The location of air cavity is significant in terms of impedance matching between the coating and water domain. Therefore, a parametric study based on the location of air cavity is done. The top and bottom radius of conical cavity is 1 and 15 mm, respectively, in this analysis. The length of the cavity is 14 mm. The distance between surface of coating and the top of conical

Table 6 Utilized element statistics (Mesh-C)

Number of elements	37,609
Minimum element quality	0.2423
Average element quality	0.6918
Element volume ratio	1.026E-4
Mesh volume	4330 mm ³

Table 5 Mesh convergences

	Mesh-A (course)		Mesh-B (medium)		Mesh-C (fine)
Number of elements	5027		18,266		37,609
Frequency (kHz)	Sound absorption coefficient	Approximately relative error (%) (A-B)	Sound absorption coefficient	Approximately relative error (%) (A-B)	Sound absorption coefficient
1	0.64452	0.19021	0.64575	0.05245	0.64609
2	0.78105	0.16892	0.77973	0.04811	0.77936
3	0.82331	0.32227	0.82067	0.09109	0.81992
4	0.83504	0.36058	0.83204	0.10175	0.83120
5	0.83325	0.32650	0.83054	0.09229	0.82977
6	0.82619	0.26192	0.82403	0.07466	0.82341
7	0.81717	0.20000	0.81554	0.05835	0.81506
8	0.80691	0.15027	0.80570	0.04783	0.80532
9	0.79674	0.12387	0.79575	0.04353	0.79541
10	0.78550	0.11054	0.78463	0.04127	0.78431

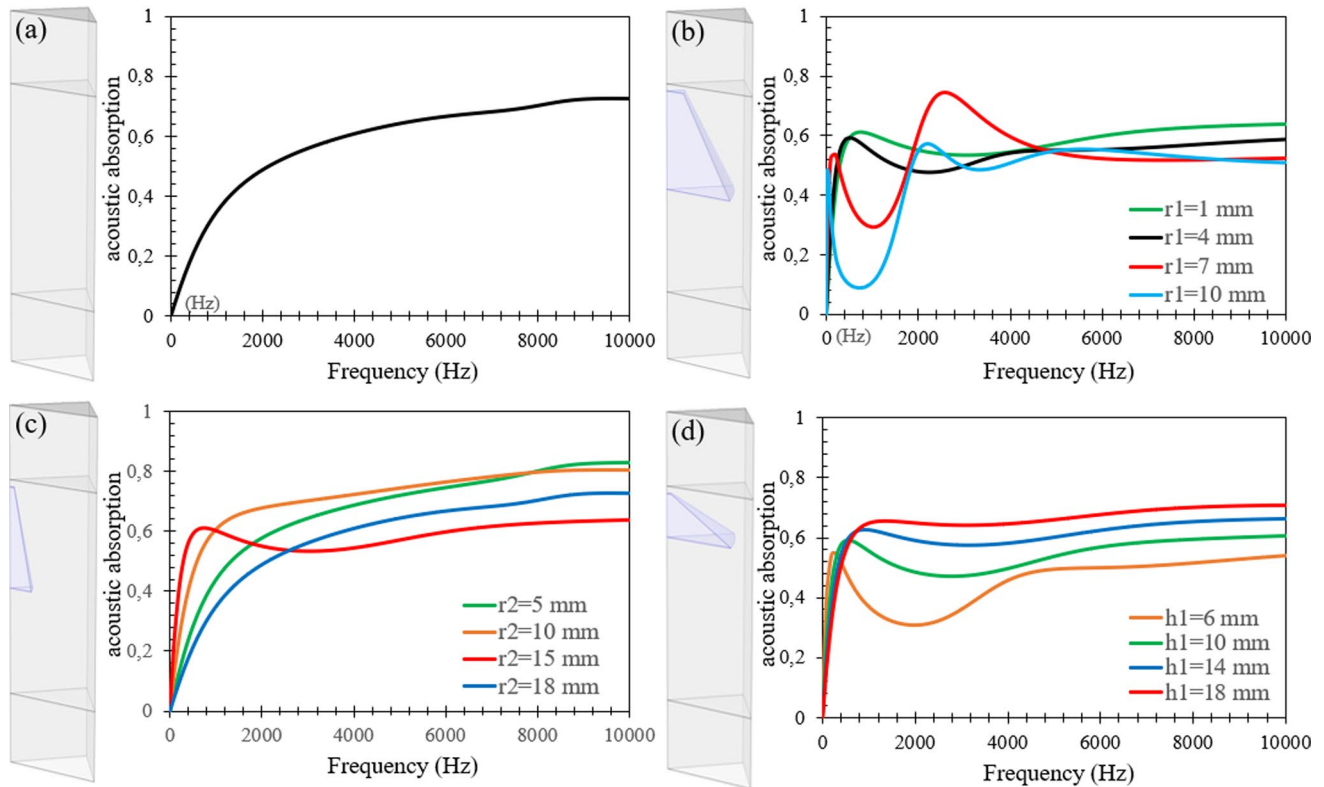


Fig. 3 **a** Pure PU, **b** top radius, **c** bottom radius, and **d** height-based optimizations

cavity is set as 1, 5, 9, and 13 mm. The results are shown in Fig. 4a. After each parameter is examined separately, top and bottom radius of conical cavity are examined together. The results are shown in Fig. 4b. Optimization studies are also carried out by reducing the dimensions of conical cavity. Firstly, all the dimensions of the cavity reduced by 20%. So, top and bottom radius are set as 0.2 and 3 mm, respectively. The length of the cavity is set as 2.8 mm, and the location of the cavity is kept constant, 1 mm below from the upper surface of coating. The results are shown as Fig. 4c. Also, the optimization of reduced conical cavity is done with parametric study. The reduced model is set as 20%, 50%, 80%, and 100% of top and bottom radius 1 and 15 mm, respectively. The length of cavity is set as 2.8 mm. The results are shown in Fig. 4d. The location of cavity is kept constant, 1 mm below the upper surface of the coating.

Also, an array designed is arranged as array with 1-mm gap horizontally and vertically. To obtain conical array, the model arranged conically in both interior and exterior geometry. The result is shown in Fig. 5a. A novel approach, which proposed in this study, is adding a traditional gong geometry as air cavity to matrix material. Gong is a traditional musical instrument, especially in Asian countries. Even when small forces are applied to this instrument, it produces very

loud sounds thanks to its high vibration feature. Sound absorption is provided by dissipated initial sound energy. The initial sound energy turns into other kind of energies such as vibration and heat. Because it turns the force into sound energy, with reverse logic, it was predicted that a gong shaped air cavity could convert sound energy into other kind of energies. The model dimensions are taken from the literature [30]. It is expected that the incident sound wave energy transforms into vibration, and heat energy thanks to gong air cavity. The technical drawing of the gong is shown in Fig. 6b. In this study, width of the coating is 40 mm; hence, the traditional gong model is not directly applicable to matrix material. Therefore, all of the dimensions of gong are offset according to width of the model proposed in this study (40 mm).

Consequently, the literature model with 112.5 mm width reduced to 15 mm with dimension of reduction ratio of 0.133; at the same time, all other dimensions are reduced according to the certain ratio. Also, a parametric study which examines the location of the gong shape cavity is done. In this analysis the distance between upper surface of gong and upper surface of coating is set as a parameter. Figure 5b shows the model and parametric study results of gong shape cavity. Moreover, the length of the gong must be reduced because the model width is 40 mm. However, the

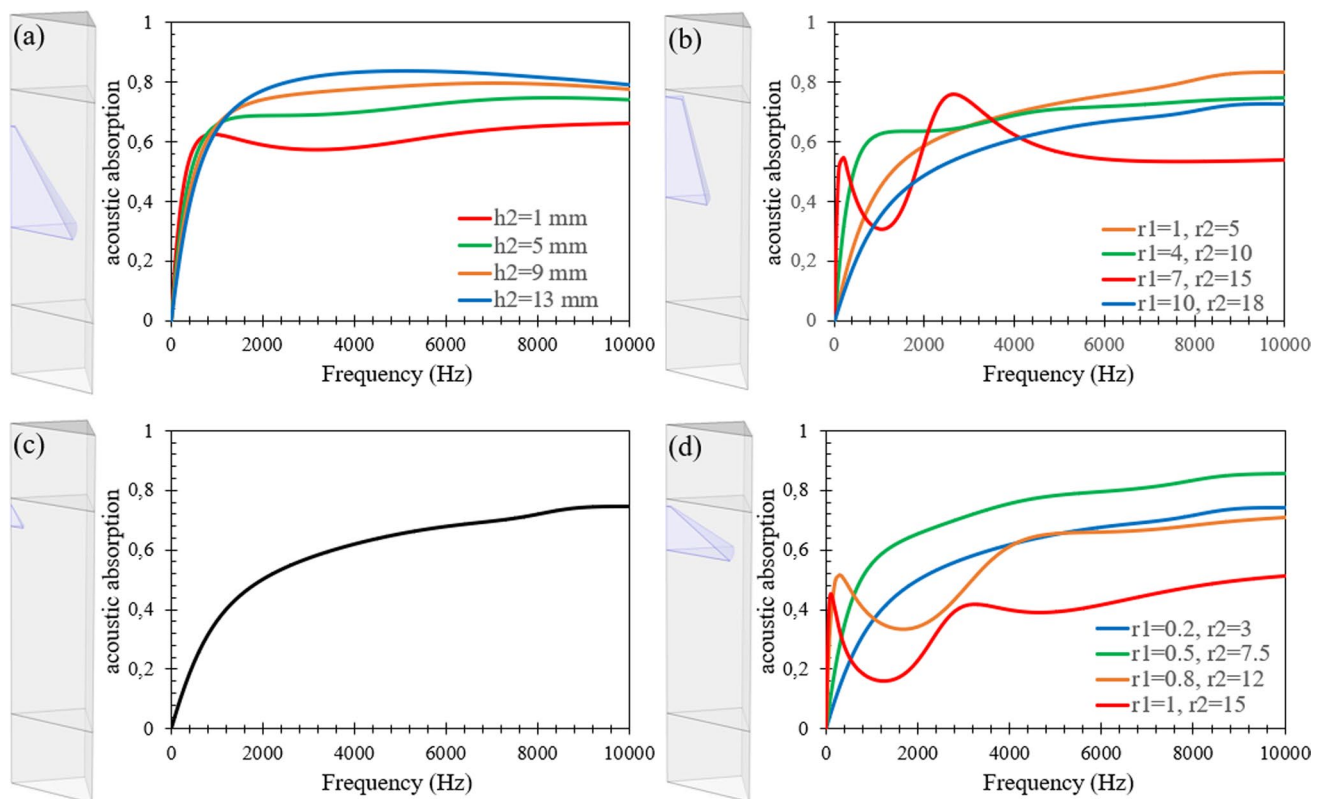


Fig. 4 **a** Conical cavity ($r_1 = 1$, $r_2 = 15$, $h_1 = 14$ mm) distance from upper surface-based optimization, **b** top-bottom radius-based optimization, **c** 80% reduced model, and **d** comparison of other reduced models (80,50, and 20% reduced models)

thickness of gong could be increased. So, the thickness of gong is set as 2 mm, and distance between the upper surface of gong and upper surface of coating is set as a parameter (h_3). Figure 5c shows the model and results of parametric study. Effect of conical cavity on acoustic performance is observed. Therefore, it is aimed to enhance its performance by designing novel gradient cavity. Sandglass model is firstly introduced. The model is arranged as arrays no gap in vertically and 1 mm gap horizontally. Moreover, a parametric study is done to determine effect of number of sandglasses. Firstly, 25 sandglasses are designed as shown in Fig. 7. After, 25, 22, 18, 13 sandglasses models are analyzed. The acoustic performance of the models is shown in Fig. 5d.

The parametric studies based on conical air cavity dimensions and location are examined with/without gong shape air cavity. To observe effect of gong, conical air cavity with $r_1 = 1$ mm, and $r_2 = 15$ mm are examined with/without gong shape air cavity ($h_3 = 22$ mm) and are shown in Fig. 8a. For bottom radius, $r_2 = 5$ mm is selected, and results are shown in Fig. 8b. For cavity length, $h_1 = 6$ mm is selected, and results are shown in Fig. 8c. For combined parametric study based on top-bottom radius the critical values are selected as $r_1 = 7$ mm, and $r_2 = 15$ mm, and results are shown in Fig. 8d.

In the low-frequency range, especially, under 100 Hz, the conical air cavity ($r_1 = 10$, $r_2 = 15$, $h_1 = 14$, $h_2 = 1$ mm) model shows good absorption performance. However, its performance decreases over 100 Hz; also fluctuations occur along 3 kHz. The performance of the conical cavity ($r_1 = 0.8$, $r_2 = 12$, $h_1 = 2.8$ mm, $h_2 = 1$ mm) has also fluctuated. The 22 sandglasses model with a gong ($h_3 = 22$ mm) shows good absorption after 600 Hz, and their performance tends to increase along 3 kHz. The conical cavity ($r_1 = 1$, $r_2 = 15$, $h_1 = 14$, and $h_2 = 1$ mm) and just gong shape cavity ($h_3 = 22$ mm) are better in terms of stability; also at lower frequencies above 600 Hz, its performance is in the middle of all models that could be shown in Fig. 9.

In the middle-frequency range, the critical models are selected again, as shown in Fig. 10. All selected critical models in this region show stable absorption performance; there are small fluctuations which could be ignored. The performance of the 25 sandglasses model with gong shape cavity ($h_3 = 22$ mm) is the best one along 3–6 kHz. The gong shape cavity model ($h_3 = 22$ mm), and 80% reduced conical cavity array with gong shape cavity ($h_3 = 22$ mm) show similar results over 4.5 kHz, but under this value, the performance of the gong shape cavity model ($h_3 = 22$ mm) is better. The 18 sandglasses model and the conical cavity

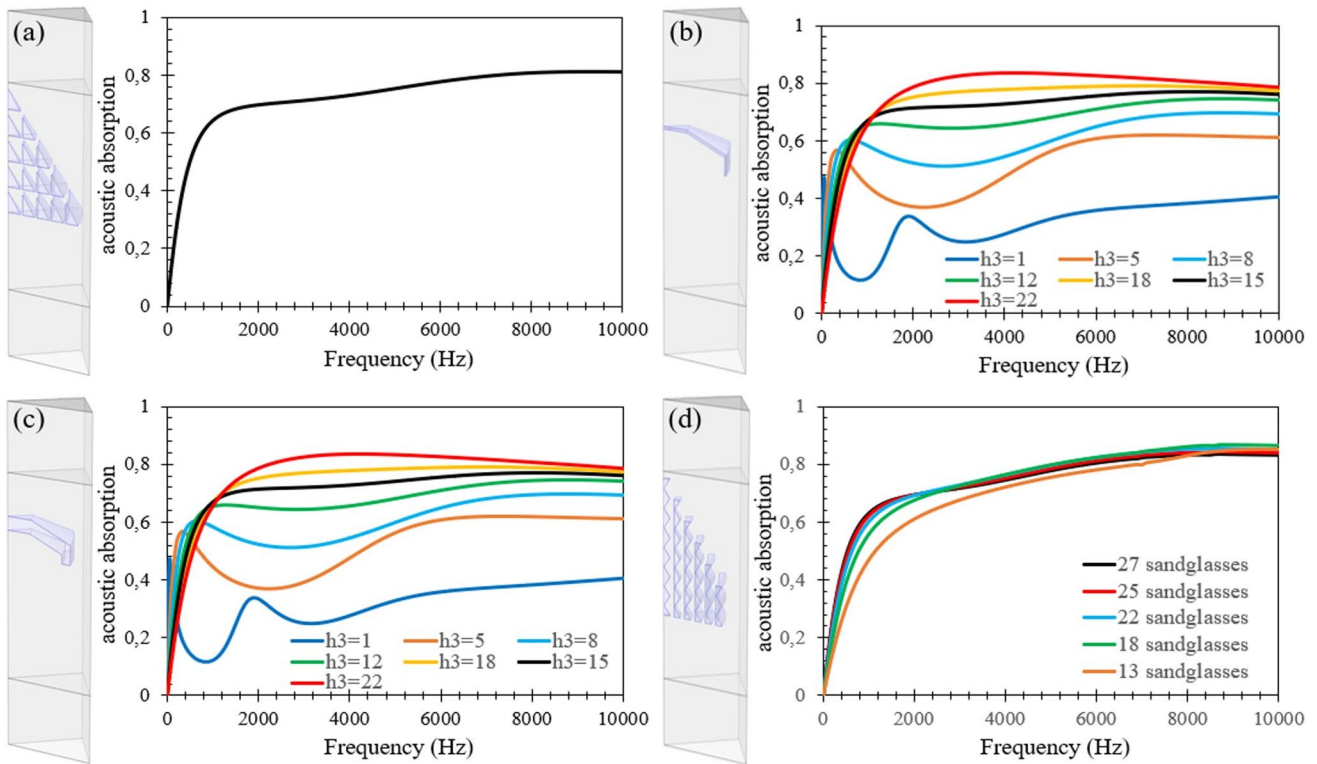
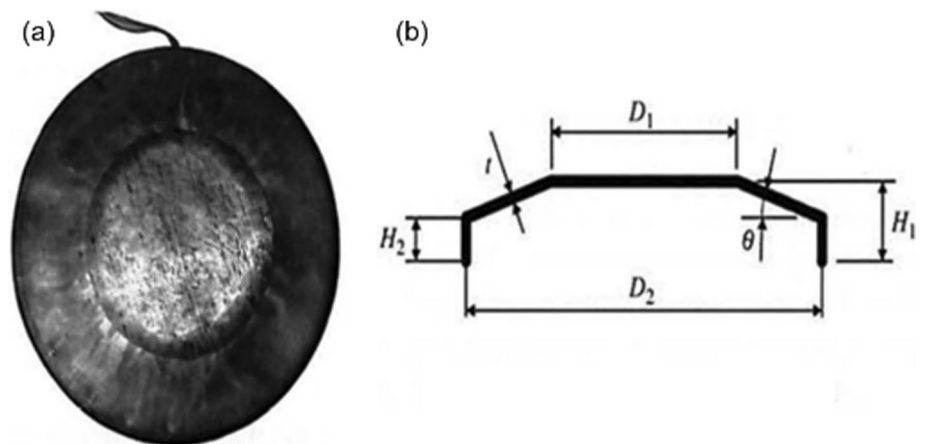


Fig. 5 **a** Reduced conical air cavity array, **b** gong shaped air cavity distance from upper surface-based optimization, **c** increased thickness gong shaped air cavity distance from upper surface-based optimization, and **d** sandglasses models

Fig. 6 **a** A traditional gong, **b** its technical drawing



($r_1 = 1$, $r_2 = 10$, $h_1 = 14$ mm, $h_2 = 1$ mm) model are similar along 3–6 kHz. Also, the conical cavity ($r_1 = 1$, $r_2 = 15$, $h_1 = 18$ mm, $h_2 = 1$ mm) shows a little lower performance than the other critical models.

The third region is between 6 and 10 kHz, the critical models are selected, and their acoustic absorption performances are shown in Fig. 11. All models show similar performances between 0.75 and 0.89. However, the performance of the 25 sandglasses model with gong shape

cavity ($h_3 = 22$) is better than the others along 6–10 kHz. The conical cavity ($r_1 = 1$, $r_2 = 5$, $h_1 = 14$, and $h_2 = 1$ mm) shows lower performance than others under 7.8 kHz, but it is in a narrow range and could be ignored (Fig. 12).

High and stable acoustic performance is observed in gong shape cavity, especially above 3.6 kHz; also it has the lowest cavity volume. On the other hand, conical cavity model achieves high acoustic performance in low frequencies; also it has the highest cavity volume.

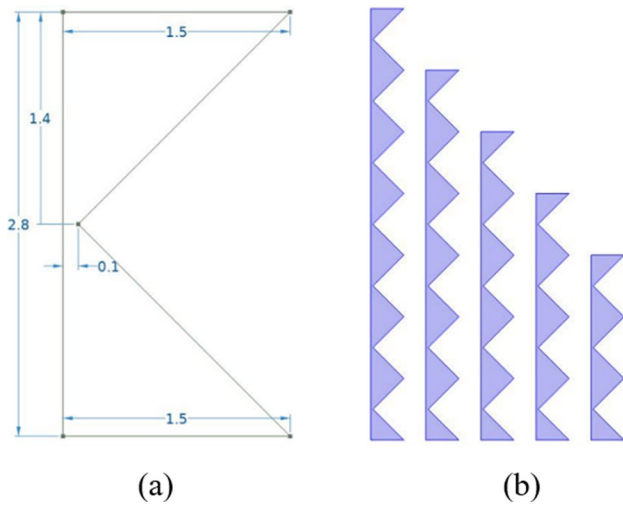


Fig. 7 **a** Sandglass unit cell dimensions (mm), **b** the model interior geometry with 25 sandglasses

The pure PU model does not contain any cavity, and this situation highly affects the deformation conditions. Due to these reasons, gong shape cavity ($h3 = 22$ mm) model, Fig. 13c,f,i, conical cavity model, Fig. 13a,d,g, and pure

PU model, Fig. 13b,e,h, are considered. The magnitude of deformation changes by the frequency. To specify a certain frequency value for the deformation analyses, acoustic performance of the models is considered. Maximum absorption performance difference is determined between pure PU, gong shape cavity, and conical cavity models. The difference between pure PU and gong shape models is 0.303 (B1-B2) at 1.3 kHz, between pure PU and conical cavity models is 0.373 (A1-A2) at 0.5 kHz, between conical cavity and gong shape cavity is 0.253 (C1-C2) at 3.6 kHz. Therefore, 0.5 kHz, 1.3 kHz, and 3.6 kHz are determined as key points. Figure 12 shows the maximum performance differences between the models. As shown as Fig. 13, highest deformation values are observed at 0.5 kHz, 1.3 kHz, and 3.6 kHz, respectively. It was observed that cavities increase the deformation magnitudes and directs to a specific region. The initial acoustic energy turns into vibration and heat energy, and vibration is the main cause of deformation rate. Hence, the acoustic absorption performance is related to the deformations. High deformation rates in broad field could be considered high acoustic performance. At 0.5 kHz and 1.3 kHz, cavities increase and concentrate deformations on a particular region compared with the pure PU model. At 3.6 kHz,

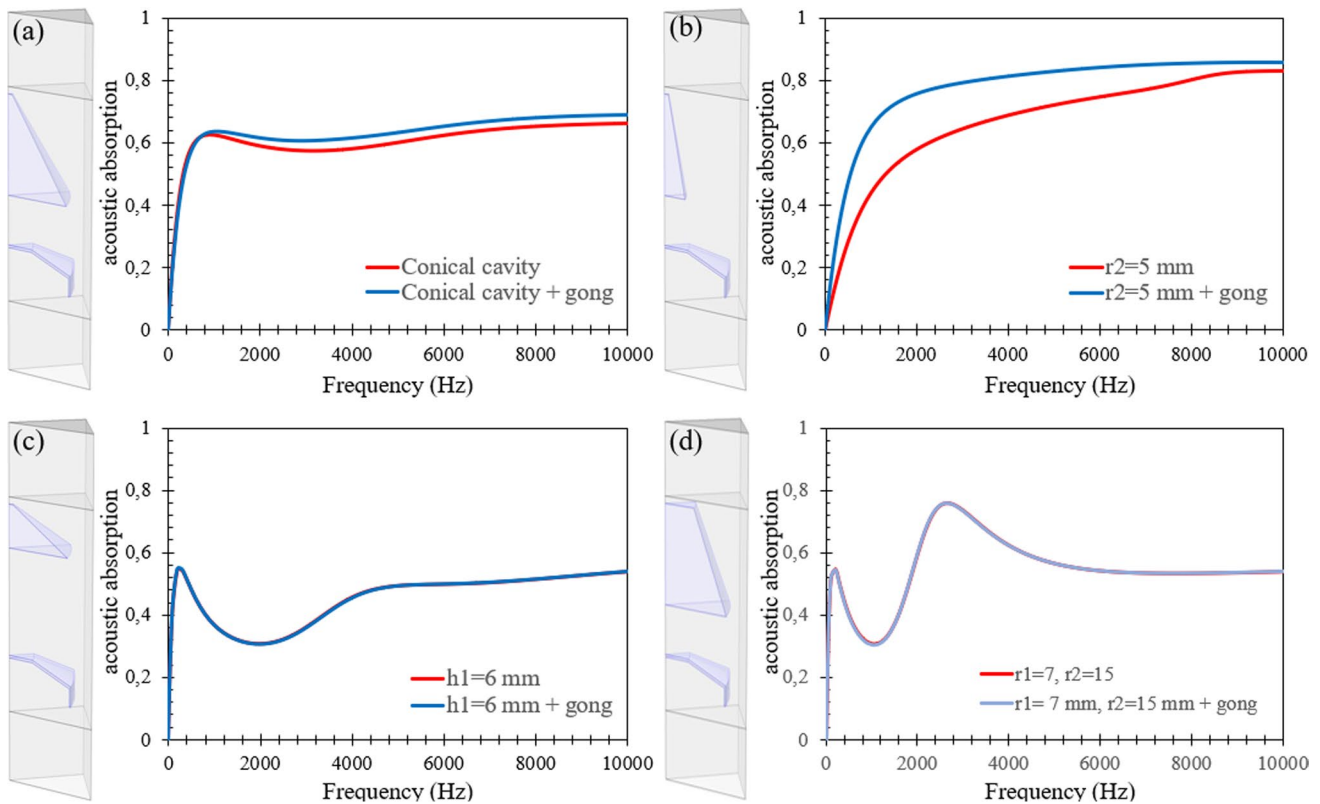


Fig. 8 **a** Conical cavity ($r1 = 1, r2 = 15, h1 = 14$ mm) with/without gong, **b** conical cavity ($r1 = 1, r2 = 5, h1 = 14$ mm) with/without gong, **c** conical cavity ($r1 = 1, r2 = 15, h1 = 6$ mm) with/without gong, and **d** conical cavity ($r1 = 7, r2 = 15, h1 = 14$ mm) with/without gong

Fig. 9 Acoustic absorption performances of the selected models in below 3 kHz

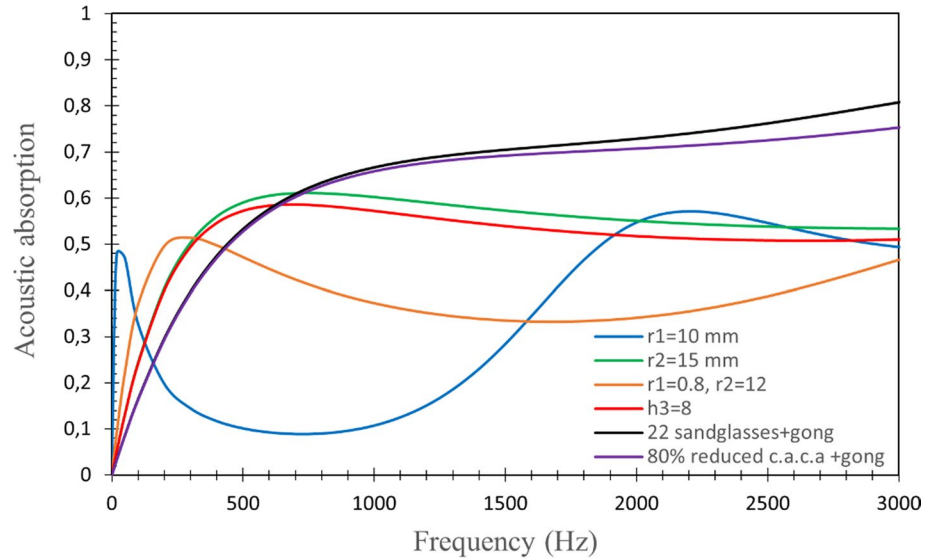
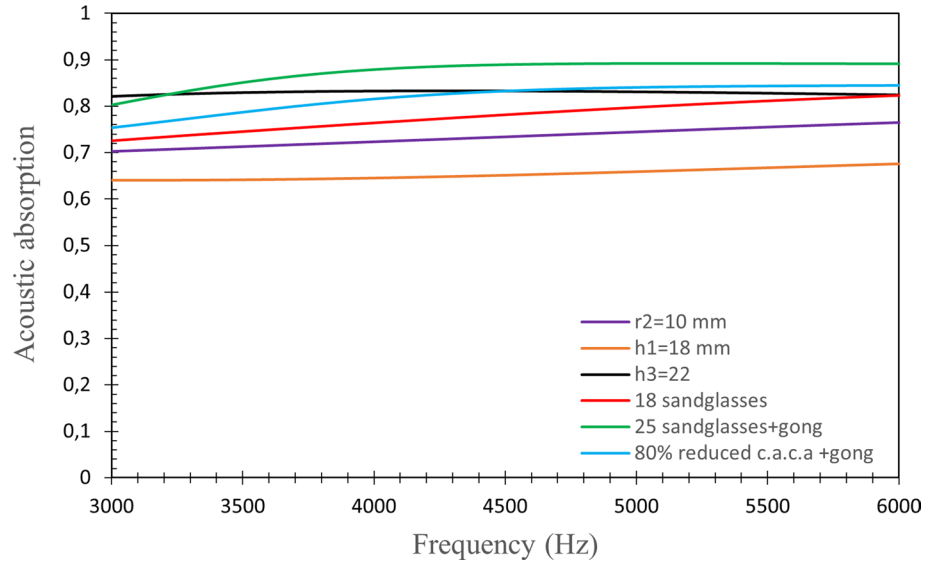


Fig. 10 Acoustic absorption performances of the selected models in 3–6 kHz



gong shape cavity model achieves higher performance and deformation rates are high at a wide area.

4 Conclusion

Acoustic metamaterials have been researched for a few decades, but most of these studies are related to air borne acoustic. Underwater acoustic metamaterials are not common as much as air borne. Nevertheless, with progressing naval technologies and their critical role in military, water-borne acoustic gains a great importance. While the underwater acoustic studies tend to military field, sonar technology has advanced. To take precautions against advanced sonar systems, underwater acoustic

metamaterial would be the first choice. However, there are still several issues that must be overcome for totally protecting from sonar systems. Firstly, absorption at low frequencies is a significant problem. Furthermore, metamaterial coating must be light, short, and resistant to hydrostatic pressure and compatible with the marine environment. Also, its absorption performance should not be limited for specific frequencies; it should provide broadband acoustic absorption.

In this study, firstly, the literature is examined and with the obtained data, a default model which consists of a matrix material (PU), steel backing (HY-80), and conical air cavity, is constructed. After, each dimension data are set as a parameter, and several parametric studies have been done. The results show that each dimension of conical

Fig. 11 Acoustic absorption performances of the selected models in 6–10 kHz

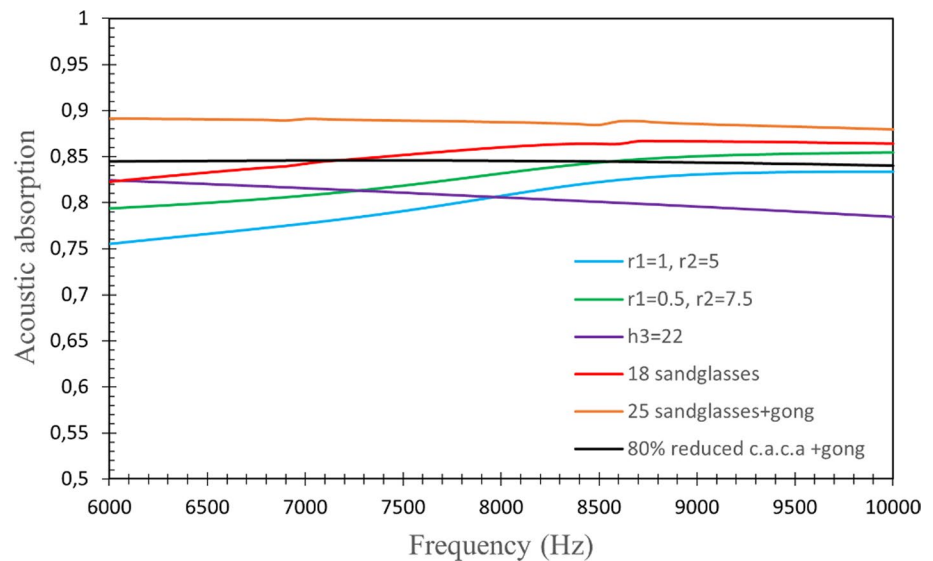
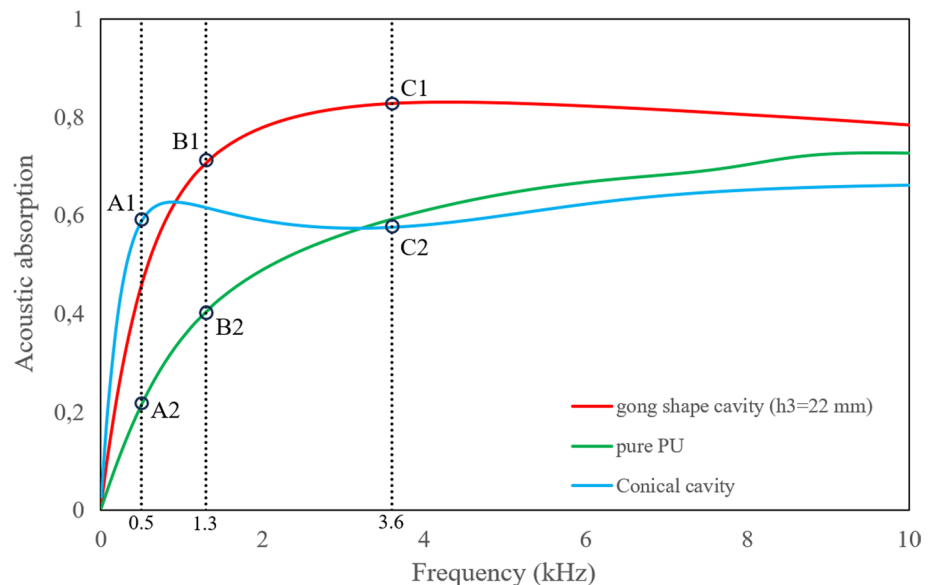


Fig. 12 Maximum absorption performance differences between the selected models



air cavity is a significant parameter ($r1, r2, h1, h2$). Also, the different combinations of these parameters affect the absorption performance significantly. Generally, at low-frequency range, acoustic performance is strongly related to air volume; increasing air volume improves the absorption performance. The location of air cavity is other significant parameter, and it is seen that increasing distance between upper surface of cavity, and lower surface of water ($h2$), improves absorption performances at middle- and high-frequency ranges. But in low-frequency range, these are opposite to each other.

Moreover, two novel approaches which proposed in this study are introduced to the matrix material. The gong shape is known with its strong vibration feature. By

changing its material from copper to air, and reducing its dimensions by a reduction coefficient, a gong shape air cavity is constructed. Its location is set as a parameter, and effect of location is examined. It is seen that while the distance between upper surface of gong and lower surface of water medium ($h3$) increases, absorption performance of gong increases at middle- and high-frequency ranges. However, at low-frequency range, the distance must be decreased to obtain high absorption performance. Also, effect of adding gong shape air cavity on other models is examined, and the results show that it increases the absorption performance of low-volume air cavities. Nevertheless, when the air cavity volume is large enough, its effect is slight. Since anechoic coatings must be used in deep waters, hydrostatic pressure is a significant factor.

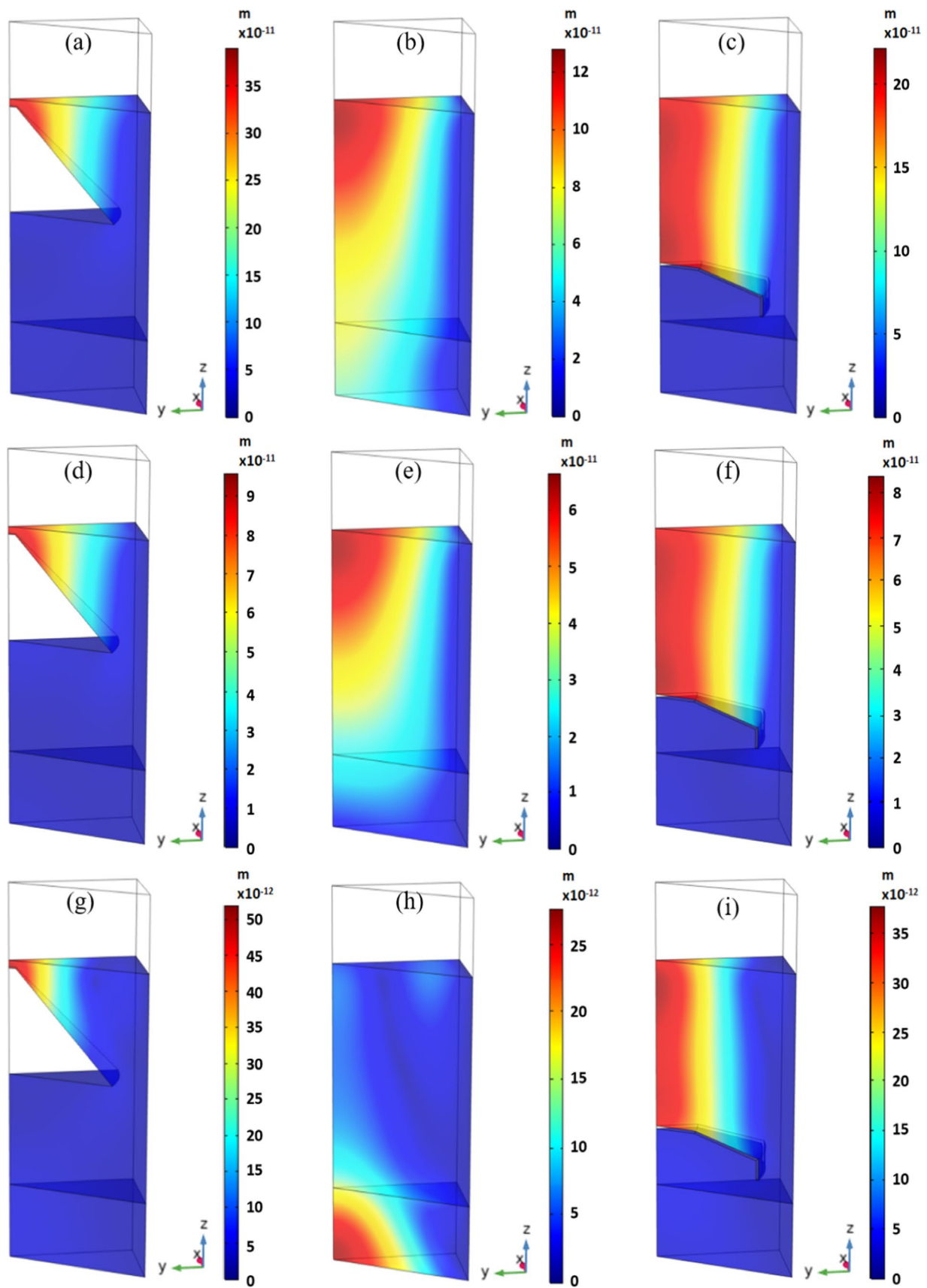


Fig. 13 Total vibration displacements at 0.5 kHz (a,b,c), 1.3 kHz (d,e,f), and 3.6 kHz (g,h,i)

Hence, air volume must be reduced as much as possible, the gong shape air cavity volume is less than other shapes. This situation is increasing its usability.

Declarations

Conflict of interest The authors have no relevant financial or non-financial interests to disclose.

Open Access This article is licensed under a Creative Commons Attribution 4.0 International License, which permits use, sharing, adaptation, distribution and reproduction in any medium or format, as long as you give appropriate credit to the original author(s) and the source, provide a link to the Creative Commons licence, and indicate if changes were made. The images or other third party material in this article are included in the article's Creative Commons licence, unless indicated otherwise in a credit line to the material. If material is not included in the article's Creative Commons licence and your intended use is not permitted by statutory regulation or exceeds the permitted use, you will need to obtain permission directly from the copyright holder. To view a copy of this licence, visit <http://creativecommons.org/licenses/by/4.0/>.

References

- Liu Z et al (2000) Locally resonant sonic materials. *Science* 289(5485):1734–1736
- Fang N et al (2006) Ultrasonic metamaterials with negative modulus. *Nat Mater* 5(6):452–456
- Kuttruff H (2016) *Room acoustics*. CRC Press
- Bobrovnikskii YI, Tomilina T (2018) Sound absorption and metamaterials: a review. *Acoust Phys* 64(5):519–526
- Ranjbar M (2011) A comparative study on optimization in structural acoustics
- Arslan H, Ranjbar M, Secgin E, Celik V (2020) Theoretical and experimental investigation of acoustic performance of multi-chamber reactive silencers. *Appl Acoust* 157:106987
- Hosseinkhani A, Younesian D, Ranjbar M, Scarpa F (2021) Enhancement of the vibro-acoustic performance of anti-tetrachiral auxetic sandwich panels using topologically optimized local resonators. *Appl Acoust* 177:107930
- Meyer E, Kuhl W, Oberst H, Skudrzyk E, Tamm K (1947) Sound absorption and sound absorbers in water. Department of the Navy, Bureau of Ships, Washington, DC, USA, Report NavShips, vol 900
- Zhao H, Wen J, Yu D, Wen X (2010) Low-frequency acoustic absorption of localized resonances: experiment and theory. *J Appl Phys* 107(2):023519
- Ivansson SM (2008) Numerical design of Alberich anechoic coatings with superellipsoidal cavities of mixed sizes. *J Acoust Soc Am* 124(4):1974–1984
- Gaunaud G (1977) One-dimensional model for acoustic absorption in a viscoelastic medium containing short cylindrical cavities. *J Acoust Soc Am* 62(2):298–307
- Wang C, Wen W, Huang Y, Chen M, Lei H, Fang D (2016) A novel broadband waterborne acoustic absorber. *AIP Adv* 6(7):075107
- Ye C, Liu X, Xin F, Lu TJ (2018) Influence of hole shape on sound absorption of underwater anechoic layers. *J Sound Vib* 426:54–74
- Gao N, Lu K (2020) An underwater metamaterial for broadband acoustic absorption at low frequency. *Appl Acoust* 169:107500
- Meng H, Wen J, Zhao H, Lv L, Wen X (2012) Analysis of absorption performances of anechoic layers with steel plate backing. *J Acoust Soc Am* 132(1):69–75
- Wang T, Liu J, Chen M (2021) Underwater sound absorption of a meta-absorption layer with double negativity. *Appl Acoust* 181:108182
- Yang H, Zhao H, Yin J, Wen J (2019) Hybrid meta-structure for broadband waterborne sound absorption. *AIP Adv* 9(12):125226
- Jin G, Shi K, Ye T, Zhou J, Yin Y (2020) Sound absorption behaviors of metamaterials with periodic multi-resonator and voids in water. *Appl Acoust* 166:107351
- Meng H, Wen J, Zhao H, Wen X (2012) Optimization of locally resonant acoustic metamaterials on underwater sound absorption characteristics. *J Sound Vib* 331(20):4406–4416
- Wang LB, Ma CZ, Wu JH (2021) A thin meta-structure with multi-order resonance for underwater broadband sound absorption in low frequency. *Appl Acoust* 179:108025
- Fu Y, Kabir II, Yeoh GH, Peng Z (2021) A review on polymer-based materials for underwater sound absorption. *Polym Testing* 96:107115
- Sperling LH (1990) *Sound and vibration damping with polymers: Basic viscoelastic definitions and concepts*. ACS Publications
- Irvine T (2004) *Damping properties of materials*. *Magnesium* 5000(3100):10–14
- Xia T, Yuwen H, Lin N (2018) Self-bonding sandwiched membranes from PDMS and cellulose nanocrystals by engineering strategy of layer-by-layer curing. *Compos Sci Technol* 161:8–15
- Crawford DM, Escarsega JA (2000) Dynamic mechanical analysis of novel polyurethane coating for military applications. *Thermochim Acta* 357:161–168
- Gao N, Zhang Y (2019) A low frequency underwater metastructure composed by helix metal and viscoelastic damping rubber. *J Vib Control* 25(3):538–548
- Atkinson RD, Wial H (2008) *Boosting productivity, innovation, and growth through a National Innovation Foundation*. Brookings-ITIF
- Qian C, Li Y (2017) Review on multi-scale structural design of submarine stealth composite. In: *Proceedings of the 2017 2nd International Conference on Architectural Engineering and New Materials*, Guangzhou, China, 2017, pp 25–26
- Bai H, Zhan Z, Liu J, Ren Z (2019) From local structure to overall performance: an overview on the design of an acoustic coating. *Materials* 12(16):2509
- Tsai GC, Wang BT, Lee YS, Chang ZW (2005) Study of vibration and sound characteristics of a copper gong. *J Chin Inst Eng* 28(4):713–719

Publisher's Note Springer Nature remains neutral with regard to jurisdictional claims in published maps and institutional affiliations.